ACS Macro Letters

Letter

pubs.acs.org/macroletters

Cascade Molecule–Particle–Molecule Self-Assemblies for Fabricating Narrowly Size-Distributed Polymeric Superparticles with a Bicontinuous Nanostructure

Yong Gao, Yafen Wang, Ming Jiang, and Daoyong Chen*

State Key Laboratory of Molecular Engineering of Polymers and Department of Macromolecular Science, Fudan University, Shanghai 200433, China

Supporting Information

ABSTRACT: Broader developments of nanoscience and nanotechnology require complexly but regularly structured nanoparticles whose fabrications in turn pose a great challenge to nanoscience and nanotechnology. In this communication, we report a new and robust method with a clear mechanism for fabricating narrowly size-distributed superparticles with a bicontinuous inner structure. The processes for the fabrication include: molecular self-assembly of a triblock copolymer in its selective solvent into the core–shell–corona micelles, the self-limited aggregation of the micelles (particles) into narrowly size-distributed superparticles constructed by the integrated micelles, and the final molecular self-assembly confined within the superparticles into cylinders that are crowded and interconnected to form the bicontinuous nanostructure; the molecular self-assembly into the micelles, the self-limited aggregation of the particles (i.e., the micelles), and the further molecular self-assembly within the superparticles occurred in a cascade manner.

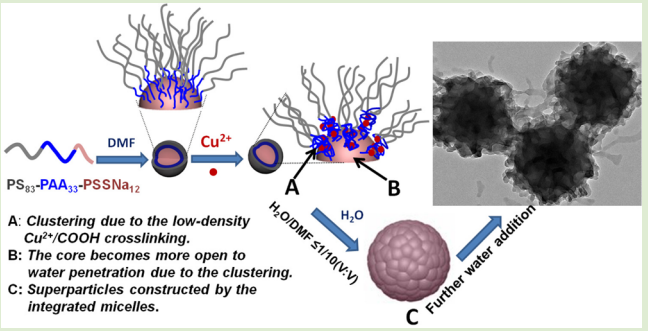

Polymeric nanoparticles play critical roles in many advanced technologies including colloidal crystals, microelectronics, controlled drug delivery, and immunoassays.[1−5] The nanoparticles for these applications are usually simply structured polymeric nanoparticles, such as uniform spheres, core–shell micelles, and bilayer nanoaggregates.[5−10] Recently, broader developments of nanoscience and nanotechnology require complexly but regularly structured nanoparticles whose fabrications in turn pose a great challenge to nanoscience and nanotechnology. These nanoparticles include multicompartment wormlike micelles, multilayer spheres, porous spheres, and the nanoparticles with bicontinuous nanostructures.[11−21] As one kind of the nanoparticles with complex but regular nanostructures, the bicontinuously structured polymeric nanoparticles (BSPNPs) are more delicately structured and are promising in the applications as nanotemplates for biomimetic mineralization, highly efficient microreactors for interfacial chemical reactions, and unique nanovehicles for controlled drug release. It was reported that self-assembly of the double-comb diblock copolymer[20] or the semicrystalline comblike block copolymer[21] could lead to BSPNPs. However, the existing methods rely on trial-and-error procedures with unclear mechanism, and the methods available for preparing BSPNPs are quite limited.

Recently, as a newly emerging scientific area, particle self-assembly has attracted much attention, as it can lead to superparticles which are expected to exhibit collective or synergistic properties and promising applications.[22−24] Constructed by nanoparticles as building blocks, superparticles are large enough to have complex but regular nanostructures, and the nanostructures can be controlled through adjusting the structure parameters of and the packing between the building blocks and/or the subsequent molecular self-assembly within the superparticles.[22] Therefore, particle self-assembly opens a new avenue for fabricating complexly but regularly structured superparticles. Herein, we report cascade molecule–particle–molecule self-assemblies for fabricating the BSPNPs formed by interconnected nanocylinders. The processes include self-assembly of a triblock copolymer in its selective solvent into core–shell–corona micelles, self-limited aggregation of the micelles (particles) into superparticles, and the final molecular self-assembly confined within the superparticles into cylinders that are crowded and interconnected to form the BSPNPs (Scheme 1). This method has the following advantages: (1) The size distribution of the superparticles is narrow, which is the result of the self-limited aggregation. (2) The method is quite robust since cylinders can be commonly obtained from block copolymer self-assembly (as explained below, in the crowded nanospace, the interconnection between the cylinders is inevitable). (3) The mechanism for forming the bicontinuous structure is clear.

Received: August 14, 2012
Accepted: October 18, 2012
Published: October 22, 2012

Scheme 1. Processes for Fabricating the Superparticles with a Bicontinuous Nanostructure

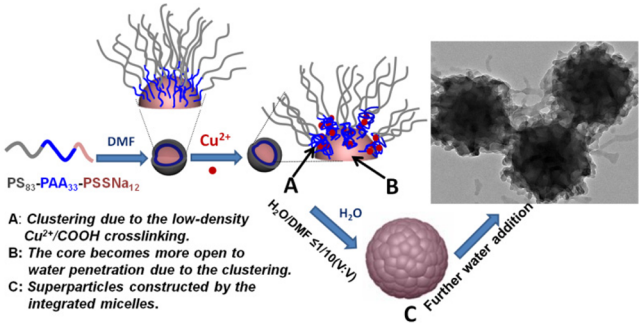

The triblock copolymer PS_{83}-b-PAA_{33}-b-$PSSNa_{12}$ (polystyrene-b-poly(acrylic acid)-b-poly(sodium 4-styrenesulfonate), the subscripts represent the average degrees of polymerization) was used for the present study (S1, Supporting Information (SI)). The molecular self-assembly of PS_{83}-b-PAA_{33}-b-$PSSNa_{12}$ in DMF at the concentration of 1.0 mg/mL led to primary micelles with an $<R_h>$ (average hydrodynamic radius) of 59 nm (Figure 1A), measured by dynamic light scattering (DLS).

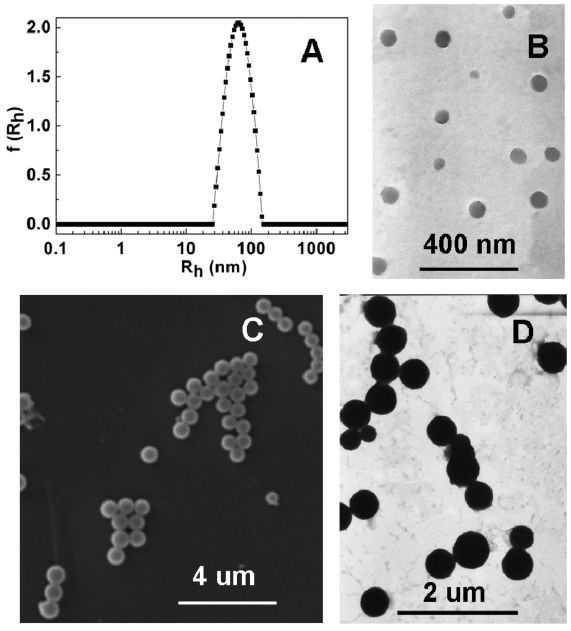

Figure 1. (A) Hydrodynamic radius distribution of the micelles in DMF. (B) TEM image of the micelles formed by PS_{83}-b-PAA_{33}-b-$PSSNa_{12}$ in DMF. (C) SEM and (D) TEM images of the superparticles formed in water.

Because DMF is a good solvent for PS and PAA but a nonsolvent for PSSNa, the micelles are with PSSNa as the core, PAA as the shell, and PS as the corona (S2 in SI). TEM observations demonstrated that the micelles are spherical with a radius about 30 nm (Figure 1B) (S3, SI), which is much smaller than the $<R_h>$; the micelles shrank during drying.

Then, neutral water was added at a rate of 0.08 mL/min into 10 mL of the micelles in DMF at 1.0 mg/mL under stirring to give the suspensions at the water/DMF volume ratios (VR) of 1:10, 1:6, 1:3, 2:3, 1:1, and 4:3, respectively. The suspension in pure water (VR = 1:0) was obtained by dialysis of the suspension at VR of 4:3 against neutral water. Due to the high hydrophobicity of the PS corona, the water addition resulted in aggregation of the micelles into superparticles, as demonstrated by DLS measurements. As indicated in Table 1, the $<R_h>$ of the

Table 1. Dependence of the $<R_h>$ of the Particles on the Water/DMF Volume Ratio (VR)

VR	0:1	1:10	1:6	1:3	2:3	1:1	4:3	1:0
$<R_h>$ (nm)[a]	59	263	251	242	234	232	230	217
$<R_h>$ (nm)[b]	53	297	287	282	293	327	326	332

[a]In the absence of Cu^{2+}. [b]In the presence of Cu^{2+} at the Cu^{2+}/COOH molar ratio of 1:50.

superparticles in the suspension at VR of 1:10 is 263 nm. Then, with a further increase in VR from 1:10 to 1:0 (pure water), the $<R_h>$ decreases steadily from 263 to 217 nm. In the SEM and TEM images, the superparticles formed at VR of 1:10 are uniform spheres with a diameter about 500 nm. Besides, when VR $\geq$ 1:10, the morphology and the size of the superparticles obtained at different VRs are similar (Figure 1C and D). Our repeated TEM and SEM observations confirm that, after VR reached 1:10, the outline of the superparticles was fixed; they neither dissociated nor aggregated with the further water addition. Therefore, the particle aggregation in the suspensions was completed before VR reached 1:10 (S4 in SI); the above-mentioned decrease in the $<R_h>$ should result from contraction of the particles caused by the increase in the water content. The aggregation of the primary micelles induced by the water addition is self-limited since it resulted in regular superparticles (Figure 1C and D). It is imaginable that the addition of water resulted in a strong attractive interaction between the primary micelles due to the high hydrophobicity of the PS corona. Meanwhile, the PSSNa block chains ionized with the water addition, and hence the micelles become negatively charged and repulsive to each other. The balance between the hydrophobic interaction and the repulsive interaction results in the self-limited aggregation; further evidence for the self-limited aggregation is discussed in S5 in SI. Self-limited aggregation of hydrophobic and charged inorganic nanoparticles into regular superparticles was reported.[25−27]

We aimed at constructing a bicontinuous nanostructure within the superparticles. It is expected that when a bicontinuous nanostructure is induced within the superparticles by the water addition all the sodium cations should be exchangeable. However, the ion exchange of the superparticles in pure water with excess strong acidic ion-exchange resin only removed 66% of the sodium ions. In these superparticles, a part of the PSSNa block chains were wrapped by the vitrified PS block chains; the sodium ions in the wrapped PSSNa block chains cannot be removed by the ion exchange experiment.

The wrapping of the PSSNa block chains by the vitrified PS corona can be avoided by adding a small amount of Cu^{2+} into the primary micelles in DMF (the molar ratio of Cu^{2+} to COOH of the PAA block is 1:50), as explained later. After the Cu^{2+} addition, the $<R_h>$ of the micelles in DMF decreased from 59 to 53 nm (Table 1). FTIR characterization confirmed the multivalent interaction between the COOH of the PAA and the Cu^{2+} (S6, SI); the $<R_h>$ decrease resulted from the noncovalent cross-linking of the PAA shell by Cu^{2+}. After the Cu^{2+} addition, neutral water was added at a rate of 0.08 mL/min into 10 mL of the micelles in DMF at 1.0 mg/mL under stirring to give the suspensions at VRs of 1:10, 1:6, 1:3, 2:3, 1:1, and 4:3, respectively. The suspension in pure water was obtained by

dx.doi.org/10.1021/mz300418b | ACS Macro Lett. 2012, 1, 1312−1316

dialysis of the suspension at a VR of 4:3 against neutral water. The superparticles with a $<R_h>$ of 297 nm formed at a VR of 1:10 (Table 1). The $<R_h>$ changes slightly in the VR range between 1:10 and 2:3. Then, the $<R_h>$ increases remarkably with a further increase in VR. The variation in $<R_h>$ with VR is different from that in the absence of Cu^{2+}. SEM and TEM observations indicate that at a VR $\leq$ 1:10 the superparticles prepared in the presence of Cu^{2+} are similar in the morphology and size to those in the absence of Cu^{2+} (data not shown). However, when VR is large, the morphology of the superparticles is quite different. As exhibited in the SEM images (Figure 2A and B), the superparticles formed in pure water and

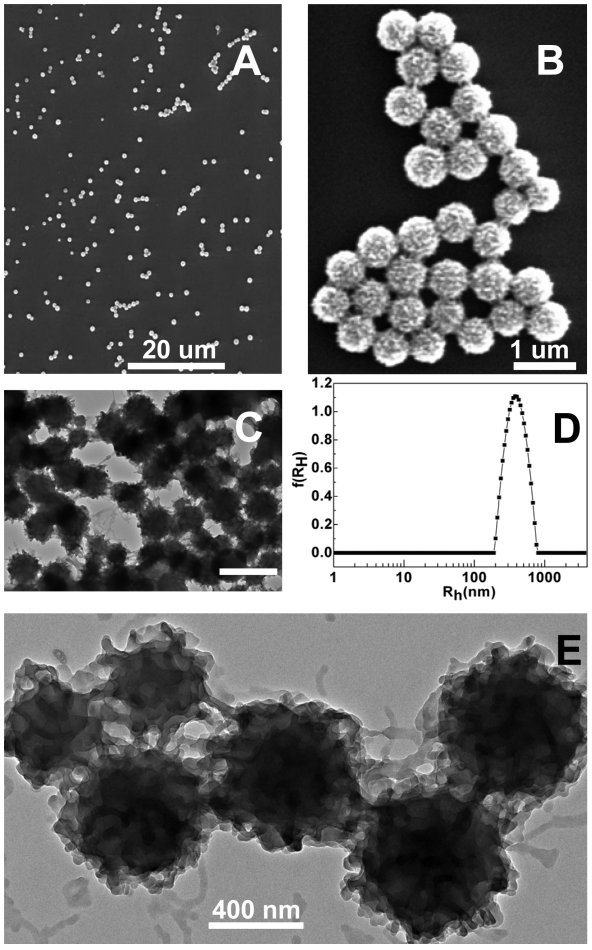

Figure 2. SEM images (A and B), TEM images (C and E), and hydrodynamic radius distribution (D) of the superparticles formed in pure water in the presence of Cu^{2+} at the Cu^{2+}/COOH molar ratio of 1:50. The scale bar in C represents 800 nm.

in the presence of Cu^{2+} are spherical and with strawberry-like morphology. The diameter of the superparticles in the SEM images is about 550 nm, and the size distribution is quite narrow (Figure 2A and B). TEM and DLS characterizations also revealed the narrow size distribution of the superparticles (Figure 2C and D). The average size of the superparticles observed by TEM is about 500 nm, close to the size observed by SEM. In the TEM images, there are both high contrast domains and low contrast domains within each superparticle (Figure 2C and E). The high contrast cylindrical domains are composed of the aggregated PS chains. The low contrast domains are almost empty, which were originally occupied by the water-swollen PAA and PSSNa blocks (as explained below) when the superparticles were in water and became empty after drying.

The existence of the water-swollen domains was confirmed by the remarkable contraction of the superparticles in 0.1 M KCl aqueous solution. In the TEM images of the superparticles cast from 0.1 M KCl aqueous solution, the low contrast domains visible in Figure 2 C and E almost disappear, and meanwhile the superparticles contract apparently (Figure 3A).

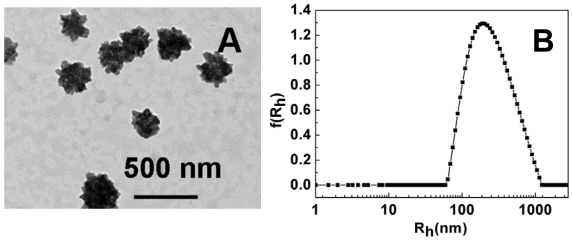

Figure 3. (A) TEM image of the superparticles formed in the presence of Cu^{2+} at the Cu^{2+}/COOH molar ratio of 1:50 after 24 h stirring in 0.1 M KCl aqueous solution. (B) DLS curve of the superparticles in 0.1 M KCl.

DLS measurements further confirmed the contraction because the $<R_h>$ of the superparticles in 0.1 M KCl decreases to 230 nm; in 0.1 M KCl aqueous solution, the polyelectrolyte chains collapsed, and thus the superparticles shrank. The $<R_h>$ changed back to 333 nm after the dialysis against pure water to remove KCl, indicating that the superparticles contracted in 0.1 M KCl can be swollen by pure water again. In 0.4 M KCl, the $<R_h>$ decreases to 209 nm, but the superparticles contracted in 0.4 M KCl cannot be swollen by the dialysis against pure water (S7, SI). It should be mentioned here that the small amount of Cu^{2+} has been removed during the dialysis of the suspension at a VR of 4:3 against neutral water to prepare the superparticles in pure water, according to atomic absorption analysis. The PS cylindrical domains should be interconnected with each other to form a continuous phase; otherwise, the swollen superparticles should have dissociated. The interconnected cylindrical structure can be seen from the TEM images with a relatively large magnification (Figure 2E). Furthermore, the superparticles formed in pure water were subjected to ionic exchange with excess strong acidic ion-exchange resin. Atomic absorption analysis confirmed that all the sodium ions in the superparticles were replaced by H^+ from the ion-exchange resin. Therefore, all the PSSNa chains were exposed to the environment outside the superparticles. The as-formed superparticles have a bicontinuous nanostructure.

As mentioned before, the outline of the superparticles was fixed at a VR of 1:10. Besides, the superparticles formed at a VR of 1:10 are actually the clusters of the primary micelles (S5 B, SI). Therefore, the further molecular self-assembly of the triblock copolymer within the superparticles at VR > 1:10 resulted in the bicontinuous nanostructure. The molecular self-assembly into the primary micelles in DMF, the self-limited aggregation of the micelles, and the further molecular self-assembly occurred in a cascade manner (S8, SI). To understand the mechanism for forming the bicontinuous structure, the system confined in the superparticles should be taken into account. For simplicity, the PAA and PSSNa blocks can be thought of as one hydrophilic block (i.e., the PAA + PSSNa hydrophilic block) because both of them are water-soluble.

dx.doi.org/10.1021/mz300418b | ACS Macro Lett. 2012, 1, 1312−1316

Considering the strong hydrophobicity of the PS block chains, the system confined within the superparticles can be considered as: a diblock copolymer in its selective solvent. The nanostructure resulting from the self-assembly within the superparticles can be predicted by the volume fraction (Φ_c) of the block copolymer in the system confined within the superparticles and the length ratio (f) of the hydrophilic block, according to the study by Yan and Shi et al.[28] In the present study, Φ_c and f were calculated to be 0.25 and 0.35, respectively (S9, SI). The stable nanostructure is cylinders (S10, SI). The formation of cylinders in the crowded confined nanospace resulted in the interconnection of the cylinders, forming the bicontinuous nanostructure. It is known that gyroid structure is usually the sole bicontinuous structure resulting from the block copolymer self-assembly. However, gyroid structure is difficult to fabricate due to the fact that it occupies a very small stable area in the phase diagram of a block copolymer in its selective solvent.[28] The method reported in the present study fabricates a bicontinuous nanostructure by forming the interconnected nanocylinders within the superparticles; the nanocylinders formed in the crowded confined nanospace are interconnected (the explanation for the interconnection is given in ref 29). This makes the method robust because, in the phase diagram, cylindrical structure occupies relatively large stable areas.[28]

Kinetically, the low-degree noncovalent cross-linking of the PAA shell by Cu^{2+} accelerated water penetration into the superparticles (Scheme 1). Theoretically, in the primary micelles formed in DMF, the PAA block chains in the shell adopt a highly stretched conformation. Thus, the Cu^{2+}/PAA complexation mainly results in interchain cross-linking. Since the molar ratio of the Cu^{2+} to the carboxyl groups of the PAA is 1:50, the cross-linking degree is low. The low degree interchain cross-linking led to the clustering of the PS and PAA block chains;[30] the PAA block chains formed clusters on the surface of the PSSNa core (Scheme 1). Due to the clustering, the PSSNa core became more open to the water penetration into the PSSNa core (Scheme 1). The clustering may also retard the aggregation of the PS block chains into an integrated vitrified corona. As the result, during the water addition, the PSSNa block chains were swollen rapidly and sufficiently to induce the phase transition, leading to the bicontinuous nanostructure.

In conclusion, PS-b-PAA-b-PSSNa forms the primary micelles in DMF. The self-limited aggregation of the micelles at the early period of the water addition led to the narrowly size-distributed superparticles, which are large enough for formation of nanostructures within them. When the PAA block chains in the primary micelles are slightly cross-linked by Cu^{2+}, the further water addition can fully swell the PSSNa block chains and induce the phase transition within the superparticles. During the phase transition, the formation of cylinders within such a crowded and confined space results in the bicontinuously structured superparticles formed by interconnected nanocylinders. This method is novel and with a clear mechanism. Besides, the method is robust since in the phase diagram cylinder structure occupies a relatively large stable area; in the crowded nanospace, the interconnection between the cylinders is inevitable.[29]

■ ASSOCIATED CONTENT

Supporting Information

Materials and methods and supplementary figures. This material is available free of charge via the Internet at http://pubs.acs.org.

■ AUTHOR INFORMATION

Corresponding Author

*E-mail: chendy@fudan.edu.cn.

Notes

The authors declare no competing financial interest.

■ ACKNOWLEDGMENTS

We are grateful for the financial support of NSFC (50825303, 91127030, and 30890140), the Ministry of Science and Technology of China (2009CB930400, 2011CB932503) and the Shanghai Committee of Science and Technology, China (11XD1400400).

■ REFERENCES

(1) de Villeneuve, V. W. A.; Dullens, R. P. A.; Aarts, D. G. A. L.; Groeneveld, E.; Scherff, J. H.; Kegel, W. K.; Lekkerkerker, H. N. W. *Science* **2005**, *309*, 1231−1233.

(2) Magbitang, T.; Lee, V. Y.; Miller, R. D.; Toney, M. F.; Lin, Z.; Briber, R. M.; Kim, H.-C.; Hedrick, J. L. *Adv. Mater.* **2005**, *17*, 1031−1035.

(3) Ha, C.-S.; Gardella., J. A., Jr. *Chem. Rev.* **2005**, *105*, 4205−4232.

(4) Montagne, P.; el-Omari, R.; Cliquet, T.; Cuilliere, M. L.; Dujeile, J. *Bioconjugate Chem* **1992**, *3*, 504−509.

(5) An, Z.; Tang, W.; Hawker, C. J.; Stucky, G. D. *J. Am. Chem. Soc.* **2006**, *128*, 15054−15055.

(6) Rao, J. P.; Geckeler, K. E. *Prog. Polym. Sci.* **2011**, *36*, 887−913.

(7) Discher, D. E.; Eisenberg, A. *Science* **2002**, *297*, 967−973.

(8) Wang, X. S.; Guerin, G.; Wang, H.; Wang, Y. S.; Manners, I.; Winnik, M. A. *Science* **2007**, *317*, 644−647.

(9) Yan, X. H.; Liu, G. J.; Liu, F. T.; Tang, B. Z.; Peng, H.; Pakhomov, A. B.; Wong, C. Y. *Angew. Chem., Int. Ed.* **2001**, *40*, 3593−3596.

(10) Blanazs, A.; Madsen, J.; Battaglia, G.; Ryan, A. J.; Armes, S. P. *J. Am. Chem. Soc.* **2011**, *133*, 16581−16587.

(11) Li, Z. B.; Kesselman, E.; Talmon, Y.; Hillmyer, M. A.; Lodge, T. P. *Science* **2004**, *306*, 98−101.

(12) Cui, H. G.; Chen, Z. Y.; Zhong, S.; Wooley, K. L.; Pochan, D. J. *Science* **2007**, *317*, 647−650.

(13) Dupont, J.; Liu, G. *Soft Matter* **2010**, *6*, 3654−3661.

(14) Fang, B.; Walther, A.; Wolf, A.; Xu, Y. Y.; Yuan, J. Y.; Müller, A. H. E. *Angew. Chem., Int. Ed.* **2009**, *48*, 2877−2880.

(15) Hales, K.; Chen, Z. Y.; Wooley, K. L.; Pochan, D. J. *Nano Lett.* **2008**, *8*, 2023−2026.

(16) Yabu, H.; Higuchi, T.; Shimomura, M. *Adv. Mater.* **2005**, *17*, 2062−2065.

(17) Saito, N.; Takekoh, R.; Nakatsuru, R.; Okubo, M. *Langmuir* **2007**, *23*, 5978−5983.

(18) Zhao, G. F.; Ishizaka, T.; Kasai, H.; Oikawa, H.; Nakanishi, H. *Chem. Mater.* **2007**, *19*, 1901−1905.

(19) Okubo, M.; Takekoh, R.; Suzuki, A. *Colloid Polym. Sci.* **2002**, *280*, 1057−1061.

(20) Parry, A. L.; Bomans, P. H. H.; Holder, S. J.; Sommerdijk, N. A. J. M.; Biagini, S. C. G. *Angew. Chem., Int. Ed.* **2008**, *47*, 8859−8862.

(21) McKenzie, B. E.; Nudelman, F.; Bomans, P. H. H.; Holder, S. J.; Sommerdijk, N. A. J. M. *J. Am. Chem. Soc.* **2010**, *132*, 10256−10259.

(22) Zhang, K. K.; Jiang, M.; Chen, D. Y. *Prog. Polym. Sci.* **2012**, *37*, 445−486.

(23) Xia, Y. S.; Tang, Z. Y. *Chem. Commun.* **2012**, *48*, 6320−6336.

(24) Xia, Y. S.; Tang, Z. Y. *Adv. Funct. Mater.* **2012**, *22*, 2585−2593.

(25) Xia, Y. S.; Nguyen, T. D.; Yang, M.; Lee, B.; Santos, A.; Podsiadlo, P.; Tang, Z. Y.; Glotzer, S. C.; Kotov, N. A. *Nat. Nanotechnol.* **2011**, *6*, 580−587.

(26) Yang, Y. S.; Meyer, R. B.; Hagan, M. F. *Phys. Rev. Lett.* **2010**, *104*, 258102−1−4.

(27) Yu, L. W.; Chen, K. J.; Song, J.; Xu, J.; Li, W.; Li, X. F.; Wang, J. M.; Huang, X. F. *Phys. Rev. Lett.* **2007**, *98*, 166102.

(28) Suo, T. C.; Yan, D. D.; Yang, S.; Shi, A. C. *Macromolecules* **2009**, *42*, 6791−6798.
(29) It is known that self-assembly of a block copolymer in its selective solvent should be carried out at a low concentration of the block copolymer. In most cases, the concentration of the block copolymer is lower than or equal to 1%; otherwise, irregular aggregates will be produced. The irregular aggregates actually result from the interconnection of the assemblies when the concentration is relatively high. In the present study, the volume fraction (c) of the block copolymer in the system confined within the superparticles is as high as 25%. Therefore, the interconnection among the nanocylinders is inevitable.
(30) Wang, Y. H.; Collins, A.; Guo, L.; Smith-Dupont, K. B.; Gai, F.; Svitkina, T.; Janmey, P. A. *J. Am. Chem. Soc.* **2012**, *134*, 3387−3395.